

# Characterization and Mechanism Elucidation of Dye Adsorption Using Cuprous Selenide Nanoparticles from Aqueous Solutions

LI Qingyan<sup>1</sup>, LIU Zhou<sup>1</sup>, HUANG Lingyan<sup>1</sup>, TENG Jiuwei<sup>2</sup> and BAI Yan<sup>1\*</sup>

1. Department of Chemistry, 2. Department of Food Science & Engineering,  
Jinan University, Guangzhou 510632, P. R. China

**Abstract** The removal of cationic dyes, methylene blue(MB) and rhodamine B(RB), and anionic dyes, methyl orange(MO) and eosin Y(EY), from aqueous solutions by adsorption using Cu<sub>2</sub>Se nanoparticles(Cu<sub>2</sub>SeNPs) was studied. The effects of the initial pH values, adsorbent doses, contact time, initial dye concentrations, salt concentrations, and operation temperatures on the adsorption capacities were investigated. The adsorption process was better fitted the Langmuir equation and pseudo-second-order kinetic model, and was spontaneous and endothermic as well. The adsorption mechanism was probably based on the electrostatic interactions and  $\pi$ - $\pi$  interactions between Cu<sub>2</sub>SeNPs and dyes. For an adsorbent of 0.4 g/L of Cu<sub>2</sub>SeNPs, the adsorption capacities of 23.1(MB), 22.9(RB) and 23.9(EY) mg/g were achieved, respectively, with an initial dye concentration of 10 mg/g(pH=8 for MB and pH=4 for RB and EY) and a contact time of 120 min. The removal rate of MB was still 70.4% for Cu<sub>2</sub>SeNPs being reused in the 5th cycle. Furthermore, the recycled Cu<sub>2</sub>SeNPs produced from selenium nanoparticles adsorbing copper were also an effective adsorbent for the removal of dyes. Cu<sub>2</sub>SeNPs showed great potential as a new adsorbent for dyes removal due to its good stability, functionalization and reusability.

**Keywords** Cu<sub>2</sub>Se nanoparticles; Adsorption; Dye

## 1 Introduction

Dyes are widely used in printing, leather, cosmetics, petroleum, food processing, rubber, and other industries<sup>[1]</sup>. At present, the total dye consumption is more than 10000 tonnes per year and approximately 100 tonnes of dyes is annually discharged into water streams<sup>[2]</sup>. The wastewater containing water-soluble dyes can cause serious environmental pollution. Even worse, most of organic dyes are harmful to human health because of their potential mutagenic and carcinogenic effects. Therefore, their removal from wastewater is urgent and related researches have attracted worldwide concerns<sup>[3]</sup>. Many innovative methods have been continuously developed to remove dyes from aqueous solution, such as biological treatment<sup>[4]</sup>, chemical oxidation<sup>[5]</sup>, ion exchange<sup>[6]</sup> and photocatalytic degradation<sup>[7,8]</sup>. However, the applications of these methods suffer from major problems of high cost and high energy consumption<sup>[9]</sup>. Adsorption is a promising method for the treatment of dyes due to its high efficiency, relative low-cost, high flexibility in design and operation<sup>[10]</sup>. Therefore, the demands for proper adsorbents have promoted searching for environmental friendly and low-cost materials among world-wide environmental scientists. In recent years, a great deal of studies have been focused on nano-adsorbents<sup>[11]</sup>, magnetic nanoparticles<sup>[12,13]</sup>, MgO@mesoporous silica spheres<sup>[14]</sup>

etc. Nano-adsorbents which have large surface areas and small diffusion resistances have shown good absorption capacity for dyes.

Recently, our group has reported that selenium nanoparticles could adsorb copper and the adsorption product was Cu<sub>2</sub>Se nanoparticles(Cu<sub>2</sub>SeNPs)<sup>[15,16]</sup>, which prompted us to study on the recycle of Cu<sub>2</sub>SeNPs. We found that those Cu<sub>2</sub>SeNPs were modified by ascorbic acid and would be negatively charged at pH above 5, and more importantly, the interaction forces between Cu<sub>2</sub>SeNPs and ascorbic acid were strong. Is it possible to remove cationic dyes by adsorption on Cu<sub>2</sub>SeNPs? In addition to electrostatic interaction, are there any other forces between Cu<sub>2</sub>SeNPs and dyes? Since the adsorption product(recycled Cu<sub>2</sub>Se nanoparticles, denoted Re-Cu<sub>2</sub>SeNPs) obtained under complicated adsorption process, it would have different particle sizes, various levels of residual ions and other molecules from the adsorption system, and thus different adsorption performance. So, it is desirable to use as-synthesized Cu<sub>2</sub>SeNPs for the investigation of the characteristics and mechanism of dye adsorption. Meanwhile, the adsorption performance of Re-Cu<sub>2</sub>SeNPs for dyes was also tested.

Herein, Cu<sub>2</sub>SeNPs modified with ascorbic acid were used as an adsorbent for the removal of water-soluble dyes. Interestingly, Cu<sub>2</sub>SeNPs could effectively adsorb both cationic and anionic dyes by electrostatic interaction and  $\pi$ - $\pi$  interaction and

\*Corresponding author. E-mail: tbaiyan@jnu.edu.cn

Received March 28, 2016; accepted June 6, 2016.

Supported by the National Natural Science Foundation of China(No.21075053).

© Jilin University, The Editorial Department of Chemical Research in Chinese Universities and Springer-Verlag GmbH

displayed good efficiency for the dye removal. In particular, the recycled Cu<sub>2</sub>SeNPs produced from selenium nanoparticles adsorbing copper could continue to be used to remove dyes from aqueous solutions. Since many molecules with specific functional groups could be used as modifiers of Cu<sub>2</sub>SeNPs, Cu<sub>2</sub>SeNPs may be useful for the removal of many other hazardous materials in the future.

## 2 Experimental

### 2.1 Materials and Methods

All the chemicals, including selenium dioxide, ascorbic acid(Vc), copper sulfate, hydrochloric acid, sodium hydroxide, methylene blue(MB), rhodamine B(RB), methyl orange(MO) and eosin Y(EY), were analytical reagents. The solution of Vc was prepared freshly.

The *zeta* potentials of the Cu<sub>2</sub>SeNPs were observed by a Malvern Zetasizer Nano ZS particle analyzer. The concentrations of dyes left in supernatant solution were determined by a TU1900 UV-Vis spectrophotometer. The Fourier transform infrared spectra were obtained on a Nicolet 6700 Fourier transform infrared spectrometer. The color of aqueous solutions containing dyes was measured by a GDYS-201M water quality multi-parameter monitor.

### 2.2 Preparation of Adsorbent

The Cu<sub>2</sub>SeNPs were prepared following procedures described in our previous work<sup>[17]</sup>. The molar ratio of Vc/CuSO<sub>4</sub>/selenium nanoparticles was 5:4:1. The XRD pattern of the Cu<sub>2</sub>SeNPs was consisted with the standard literature data (JCPDS No. 88-2043). The recycled Cu<sub>2</sub>Se nanoparticles were the adsorption products obtained by adsorption of Cu(I) onto the selenium nanoparticles<sup>[15]</sup>. The Re-Cu<sub>2</sub>SeNPs were collected together from dialysis bags, washed repeatedly with deionized water and dried at 60 °C for 24 h for further use.

### 2.3 Batch Adsorption Experiments

Taking MB as an example, the adsorption experiments were described as following, a similar procedure was followed for other dyes. The Cu<sub>2</sub>SeNPs were mixed with 50.0 mL of MB solution and then the mixture was stirred on a magnetic stirring apparatus until the system reached adsorption equilibrium. The concentration of dye was determined by measuring the decrease of the dye absorbance at its maximum absorbance wavelength. The MB adsorption capacity[gram MB adsorbed

per gram of Cu<sub>2</sub>SeNPs( $Q_e$ )] is calculated according to Eq.(1), the removal rate( $R$ ) is calculated according to Eq.(2):

$$Q_e = \frac{V(c_0 - c_e)}{m} \quad (1)$$

$$R(\%) = \frac{c_0 - c_e}{c_0} \times 100\% \quad (2)$$

where  $c_0$  and  $c_e$  represent the initial and the equilibrium MB concentrations(mg/L), respectively;  $V$  is the volume of MB solution(L) and  $m$  is the mass of adsorbent(g).

The initial pH values of the dye solutions were adjusted with 0.1 mol/L NaOH or HCl using a pH meter. In regeneration of adsorbent, the Cu<sub>2</sub>SeNPs@MB and Re-Cu<sub>2</sub>SeNPs@MB were washed thoroughly with the mixture of ethanol and acetic acid(volume ratio, 4:1) and deionized water consecutively.

## 3 Results and Discussion

### 3.1 Dyes Adsorption on Cu<sub>2</sub>Se Nanoparticles

Cationic dyes(MB, RB) and anionic dyes(MO, EY) were selected as a simplified model of the water-soluble dyes to investigate the adsorption characteristics of dyes on the Cu<sub>2</sub>SeNPs. These solutions of dyes became almost clear after treated with Cu<sub>2</sub>SeNPs. As shown in Fig.1, the chromaticities of aqueous solutions containing dyes(10 mg/L) decreased to 0.4°, 0.1° and 0.9° from 40°, 20° and 60° for MB, RB and EY, respectively, which were lower than the required value in drinking water quality standard(GB T5750-2006), *i.e.*, below 15°. Further experiments showed that there were no significant difference on the removal rates of dyes in different light sources(*i.e.*, UV light and indoor light). Therefore, Cu<sub>2</sub>SeNPs removed dyes from aqueous solution resulting from their adsorption characteristics.

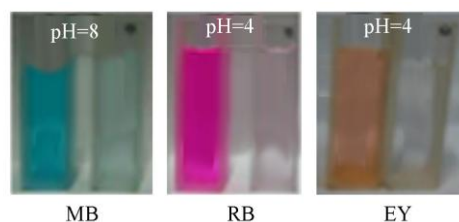


**Fig.1 Chromaticities of aqueous solutions containing dyes before(left) and after(right) adsorption**

The removal rates for different dyes are listed in Table 1. These results indicated that removal rates for dyes may be associated with the charges and their electrostatic interactions of Cu<sub>2</sub>SeNPs and dyes.

**Table 1 Removal rate and adsorption capacity of dyes on Cu<sub>2</sub>SeNPs\***

Cationic dye	pH = 8		pH = 4		Anionic dye	pH = 8		pH = 4	
	$R_t(\%)$	$Q_t(\text{mg}\cdot\text{g}^{-1})$	$R_t(\%)$	$Q_t(\text{mg}\cdot\text{g}^{-1})$		$R_t(\%)$	$Q_t(\text{mg}\cdot\text{g}^{-1})$	$R_t(\%)$	$Q_t(\text{mg}\cdot\text{g}^{-1})$
MB	88.4	23.1	76.0	18.0	MO	39.3	9.84	52.6	13.1
RB	81.5	20.4	91.4	22.9	EY	43.7	10.9	95.5	23.9

\*  $c_0 = 10.0 \text{ mg/L}$ ;  $m = 0.02 \text{ g}$ ;  $t = 120 \text{ min}$ ;  $T = 298 \text{ K}$ .

In order to investigate factors affecting dye adsorption and to obtain an insight into the adsorption mechanism of dyes on Cu<sub>2</sub>SeNPs, MB, RB and EY were selected as the representative adsorbates for the interpretation of adsorption process. To our surprise, the operation conditions made the same effects on

adsorptions of MB, RB and EY with the exception of pH values.

#### 3.1.1 Effects of pH

Based on the above findings, the adsorption of dyes was primarily affected by the surface charge of Cu<sub>2</sub>SeNPs changed

with the pH. As shown in Fig.2(A), the  $\text{pH}_{\text{pzc}}$  value (the pH at the point of zero charge) of the  $\text{Cu}_2\text{SeNPs}$  was found to be 5. The adsorption capacities of MB (cationic dye) increased from 16.6 mg/g to 23.1 mg/g with the pH values increasing from 2 to 8. In contrast, the acidic solution ( $\text{pH} < 5$ ) was favorable to the adsorption of EY (anionic dye). However, the cationic dyes (MB and RB, the initial solution  $\text{pH} < 5$ ) and anionic dyes (EY, the initial solution  $\text{pH} > 5$ ) could still adsorb on  $\text{Cu}_2\text{SeNPs}$  despite the electrostatic repulsion between the  $\text{Cu}_2\text{SeNPs}$  and dyes, which suggested that in addition to the surface charge of  $\text{Cu}_2\text{SeNP}$  and electrostatic attractions, other interaction

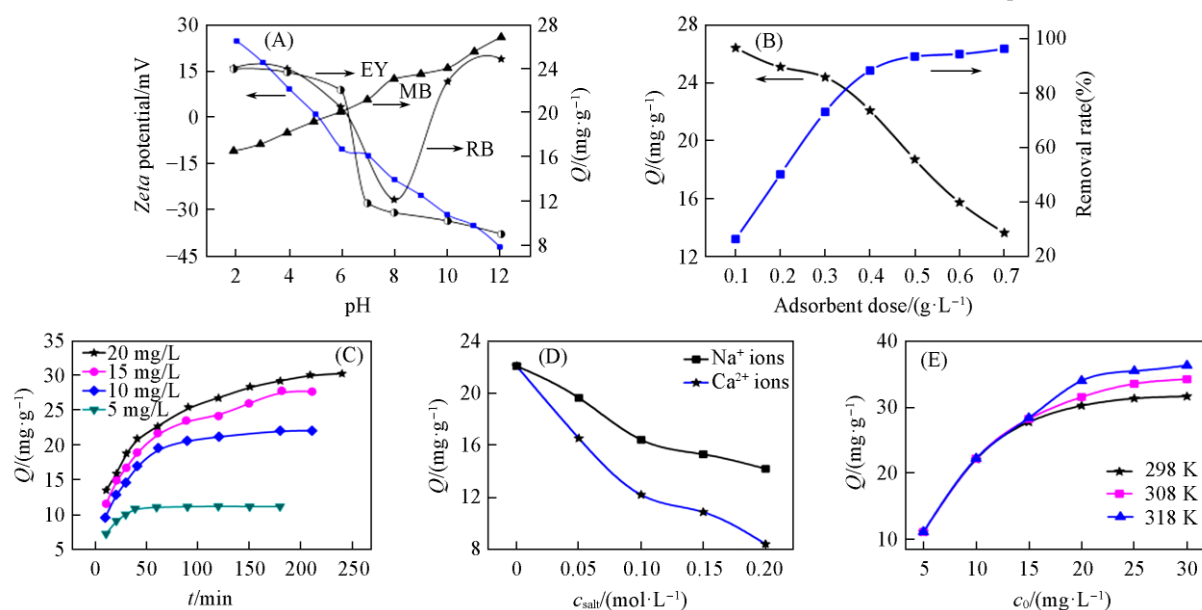


**Fig.2** Effects of zeta potentials of  $\text{Cu}_2\text{SeNPs}$  and pH values(A), adsorbent doses(B), contact time and the initial MB concentrations(C), salt concentrations(D) and temperatures(E) on the adsorption of MB on  $\text{Cu}_2\text{SeNPs}$

Experiment conditions: (A)  $c_0=10.0$  mg/L,  $m=0.02$  g,  $t=120$  min; (B), (D), (E)  $c_0=10.0$  mg/L,  $t=120$  min,  $\text{pH}=8$ ; (C)  $\text{pH}=8$ .

### 3.1.2 Effect of Adsorbent Dose

As shown in Fig.2(B), the removal rates of MB increased from 26.5% to 96.4% when the adsorbent doses increased from 0.1 g/L to 0.7 g/L, while the adsorption capacities decreased slightly from 26.5 mg/g to 13.6 mg/g. Further increase in adsorbent doses would have less effect on the removal rates of MB. These results were associated to the mass transfer limitations due to the depletion of the dye in the aqueous phase. Therefore, a dose of 0.4 g/L of  $\text{Cu}_2\text{SeNPs}$  was selected for the further experiments.

### 3.1.3 Effects of Contact Time and Initial MB Concentration

As shown in Fig.2(C), the adsorption capacities of MB drastically increased at beginning and then remained almost unchanged, indicating that the adsorption reached equilibrium. Meanwhile, the increasing magnitude of adsorption capacities was less and less with the increase of initial concentrations. In addition, the time needed to reach adsorption equilibrium shortened with decreasing initial MB concentrations. These results were attributed to the fact that most vacant surface sites were available for adsorption during the initial stage, and after a duration of time, the remaining vacant surface sites were difficult to be occupied.

between  $\text{Cu}_2\text{SeNPs}$  and dyes could also be responsible for the adsorption of dyes on the  $\text{Cu}_2\text{SeNPs}$ . According to the FTIR spectra, these results could result from  $\pi$ - $\pi$  interaction between  $\text{Cu}_2\text{SeNPs}$  and dyes (see section 3.2). Unlike MB and EY, the adsorption capacities of RB (cationic dye) were a minimum at pH 8 and maximums at pH 2 to 4 and 10. In this case, the effects of the charge on the adsorption capacities of RB cannot explain entirely the results and the adsorption of RB depended on the existing species of RB in aqueous solutions (see section 3.2). The initial solution with pH 8 for MB and pH 4 for RB and EY were selected in the further experiments.

### 3.1.4 Effects of Concentrations of NaCl and $\text{CaCl}_2$

It is well known that salts can interfere with the electrostatic interactions by the electrostatic screening effect<sup>[18]</sup>. As shown in Fig.2(D), when the concentrations of salts increased from 0 to 0.2 mol/L, the adsorption capacities of MB decreased from 23.1 mg/g to 14.2 mg/g and 8.5 mg/g for NaCl and  $\text{CaCl}_2$ , respectively, which resulted from the competitive effect between cationic ions and MB for the sites available on the adsorbent. On the other hand,  $\text{Ca}^{2+}$  ions had greater contribution to ionic strength and larger positive charges than  $\text{Na}^+$  ions, so the effect of  $\text{Ca}^{2+}$  ions on adsorption was stronger than that of  $\text{Na}^+$  ions. These results also confirmed the electrostatic interaction between the  $\text{Cu}_2\text{SeNPs}$  and dyes.

### 3.1.5 Effect of Temperature

The effects of temperatures on the adsorption of MB at different initial concentrations are presented in Fig.2(E). The adsorption capacities increased with increasing temperatures in the range of 298–318 K, suggesting that MB adsorption on the  $\text{Cu}_2\text{SeNPs}$  was endothermic in nature.

For a dose of 0.4 g/L of  $\text{Cu}_2\text{SeNPs}$ , the dye removal rates of 88.4%(MB), 91.4%(RB) and 95.5%(EY) could be achieved with an initial dye concentration of 10.0 mg/L (pH 8 for MB and pH 4 for RB and EY) and a contact time of 120 min.

### 3.2 Proposed Adsorption Mechanism

Herein, we are going to investigate the functions of the surface groups modified on Cu<sub>2</sub>SeNPs in the dye adsorption according to the information from FTIR spectra and to discuss the adsorption mechanism of dyes on Cu<sub>2</sub>SeNPs.

#### 3.2.1 Surface Modification and Functionalization of Cu<sub>2</sub>Se Nanoparticles

As shown in Fig.3(A), the FTIR spectra of the Cu<sub>2</sub>SeNPs, Re-Cu<sub>2</sub>SeNPs and Vc showed some information about characteristic functional groups. The absorption bands around 3000 to 3600, 1673 and 1131 cm<sup>-1</sup> were corresponded to —OH, C=C and C—O stretching vibration of Vc, respectively. Comparing with Vc, only a broad absorption band at 3445 cm<sup>-1</sup> indicated that the —OH vibrational degree of freedom decreased significantly in Cu<sub>2</sub>SeNPs and Re-Cu<sub>2</sub>SeNPs. The C—O stretching vibration of Cu<sub>2</sub>SeNPs and Re-Cu<sub>2</sub>SeNPs shifted to 1107 and 1069 cm<sup>-1</sup>, respectively, which related to C—O stretching vibration coordinating to Cu(I)<sup>[19]</sup>. The C=C stretching vibration of Cu<sub>2</sub>SeNPs and Re-Cu<sub>2</sub>SeNPs shifted to about 1667 cm<sup>-1</sup>. There were a modified layer of Vc on the surface of Cu<sub>2</sub>SeNPs, in which a certain amount of oxygen-containing functional groups, such as —OH, were capable of providing adsorption sites for electrostatic interactions by deprotonated at neutral or basic solutions, and C=C provide  $\pi$ - $\pi$  interaction between Cu<sub>2</sub>SeNPs and dyes. Additional, the Cu<sub>2</sub>SeNPs and Re-Cu<sub>2</sub>SeNPs modified by Vc showed the loose net structure (see the SEM image in references<sup>[17]</sup> and<sup>[15]</sup>), which play an important role in the adsorption.

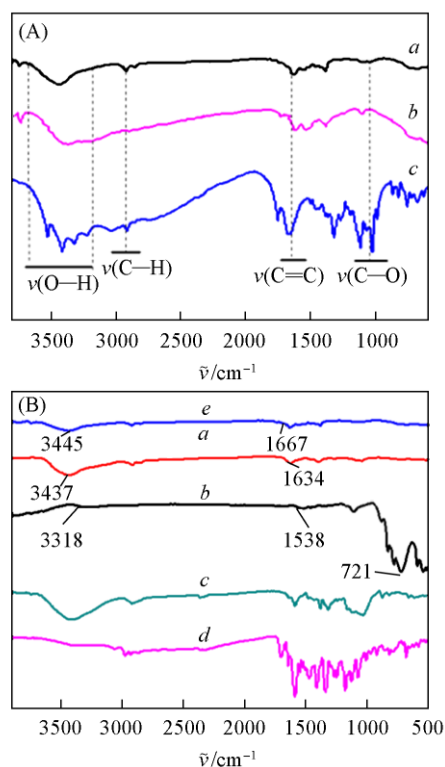


**Fig.3** FTIR spectra of Cu<sub>2</sub>SeNPs(a), Re-Cu<sub>2</sub>SeNPs(b) and Vc(c)(A), Cu<sub>2</sub>SeNPs@MB(a), Cu<sub>2</sub>SeNPs@RB(b), MB(c), RB(d) and Cu<sub>2</sub>Se(e)(B)

#### 3.2.2 Changes of Zeta Potentials and Electrostatic Attractions

From the changes of *zeta* potentials of Cu<sub>2</sub>SeNPs vs. adsorption capacities[Fig.2(A)] and Table 1, it can be concluded that cationic/anionic dyes adsorbed on Cu<sub>2</sub>SeNPs surfaces by interactions with opposite charges. When pH values were above 5, especially above 8, the adsorption capacities and the removal rates of cationic dyes increased significantly. While pH values were below 5, anionic dyes were effectively adsorbed. These results were contributed to the electrostatic attraction between the Cu<sub>2</sub>SeNPs and dyes. In fact, the deprotonated —OH on the surface of Cu<sub>2</sub>SeNPs interacted with positive charges on dyes by electrostatic attraction. In Fig.3(B), the vibrational fingerprints centered at 3445 cm<sup>-1</sup> (—OH stretching) for Cu<sub>2</sub>SeNPs notably red-shifted to 3437 cm<sup>-1</sup> for Cu<sub>2</sub>SeNPs@MB and to 3318 cm<sup>-1</sup> for Cu<sub>2</sub>SeNPs@RB), which may be associated to the electrostatic interaction between Cu<sub>2</sub>SeNPs and dyes.

#### 3.2.3 Aromatic Rings and $\pi$ - $\pi$ Interactions

When pH values were below 5, the cationic dyes, MB and RB, could still adsorb on the positively charged Cu<sub>2</sub>SeNPs despite the electrostatic repulsion between the Cu<sub>2</sub>SeNPs and dyes. It is suggested that the driving force for the adsorption of dyes would be  $\pi$ - $\pi$  interactions between the C=C bonds on the surface of Cu<sub>2</sub>SeNPs and the aromatic rings of dye molecules<sup>[3]</sup>. The FTIR spectra of Cu<sub>2</sub>SeNPs@MB(RB) and dyes provided information on the  $\pi$ - $\pi$  interactions[Fig.3(B)]. For example, the absorption band of C=C stretching vibration at 1667 cm<sup>-1</sup> (Cu<sub>2</sub>SeNPs) shifted towards lower wavenumbers(1634 cm<sup>-1</sup> for Cu<sub>2</sub>SeNPs@MB, 1538 cm<sup>-1</sup> for Cu<sub>2</sub>SeNPs@RB), which was contributed to  $\pi$ - $\pi$  interactions between the C=C bonds on surface of Cu<sub>2</sub>SeNPs and the aromatic rings of the dye. Moreover, as shown in the FTIR spectra of Cu<sub>2</sub>SeNPs@RB, a new absorption band was observed at 721 cm<sup>-1</sup>, which could originate from the =CH out-of-plane bending vibration of aromatic rings for RB<sup>[20]</sup>.

Similarly, Cu<sub>2</sub>SeNPs took on little negative charges at pH values 6 to 7[Fig.2(A)] and thus there was weak repulsion between Cu<sub>2</sub>SeNPs and anionic dyes. The higher adsorption capacities of EY(13.2 to 11.8 mg/g at pH values 6 to 7) were contributed to  $\pi$ - $\pi$  interactions. In basic solution, however, anionic dyes were difficult to close to the adsorbent because electrostatic repulsion between Cu<sub>2</sub>SeNPs and anionic dyes was too strong, leading to a remarkable decrease in the adsorption capacities of EY.

#### 3.2.4 Dimerization of RB and Adsorption Decrease

The RB adsorption was also severely affected by its dimerization. RB molecules exist as the cationic form in an aqueous solution of lower pH, and become the zwitterionic form at pH values above 4<sup>[21]</sup>. The zwitterionic form is a bigger molecular dimer formed by electrostatic attraction between the carboxyl and xanthane groups of the monomer. Compared with the cationic form, the dimer reduced the electrostatic attraction between the RB and the negatively charged Cu<sub>2</sub>SeNPs and was difficult to enter into loose net structure of Cu<sub>2</sub>SeNPs due to its bulkier molecular structure, leading to the decrease in RB

adsorption in pH range of 5–8. At pH values above 8, the excess of hydroxyl competed with carboxyl, which decreased the dimerization of RB and the RB adsorption increased with the negative shift of *zeta* potentials of Cu<sub>2</sub>SeNPs.

Based on the above discussion, the adsorption process and mechanism for the dye on Cu<sub>2</sub>SeNPs could be inferred as Fig. 4. The adsorption removal 4 dyes from aqueous solutions using Cu<sub>2</sub>SeNPs as the adsorbent was the result of the combined action of electrostatic interaction and  $\pi$ - $\pi$  interaction between Cu<sub>2</sub>SeNPs and dyes.

### 3.3 Adsorption Isotherm

The related parameters of Langmuir and Freundlich isotherms for MB adsorption on Cu<sub>2</sub>SeNPs are showed in Table 2.

**Table 2** Langmuir and Freundlich isotherms constants and correlation coefficients for MB adsorption on Cu<sub>2</sub>SeNPs\*

T/K	Langmuir					Freundlich			
	$Q_{\max}/(\text{mg}\cdot\text{g}^{-1})$	$10^3 K_L/(\text{L}\cdot\text{g}^{-1})$	$R_L$	Linear equation	$r^2$	$K_F$	$n$	Linear equation	$r^2$
298	33.3	1.229	0.0264–0.1340	$c_e/Q_e=0.03+0.03c_e$	0.999	16.8	3.77	$\ln Q_e=2.82+0.27 \ln c_e$	0.805
308	33.9	1.264	0.0257–0.1370	$c_e/Q_e=0.03+0.027c_e$	0.999	17.1	3.73	$\ln Q_e=2.83+0.29 \ln c_e$	0.795
318	34.2	1.343	0.0242–0.1300	$c_e/Q_e=0.04+0.025c_e$	0.998	17.7	3.84	$\ln Q_e=2.84+0.32 \ln c_e$	0.805

\*  $Q_e(\text{mg}/\text{g})$ : amount of MB adsorbed on the adsorbent at equilibrium;  $c_e(\text{mg}/\text{L})$ : equilibrium concentration of MB in solution;  $Q_{\max}(\text{mg}/\text{g})$ : maximum adsorption capacity;  $K_L(\text{L}/\text{g})$ : Langmuir equilibrium constant;  $K_F$  and  $n$ : Freundlich constants and adsorption intensity, respectively.

The correlation coefficients ( $r^2$ ) indicated that the Langmuir mode was suitable for describing the adsorption equilibrium of MB on Cu<sub>2</sub>SeNPs. The separation factor ( $R_L$ ) related to Langmuir isotherm is used to evaluate the feasibility of adsorption on adsorbent. It can be calculated by Eq.(3):

$$R_L = \frac{1}{1 + K_L c_0} \quad (3)$$

As shown in Table 2, the values of  $R_L$  at different initial MB concentrations and different temperatures were 0.0242 to 0.1370, within the range of 0 to 1, confirming that the adsorption of MB on Cu<sub>2</sub>SeNPs was favorable<sup>[22]</sup>. Furthermore, the values of  $n$  were 3.73 to 3.84, within the range of 1 to 10, which also provided evidence to a favorable adsorption processes<sup>[23]</sup>.

### 3.4 Thermodynamic Analysis

The changes in free energy ( $\Delta G$ ), enthalpy ( $\Delta H$ ) and entropy ( $\Delta S$ ) associated with the adsorption process are shown in Table 3. The negative values for  $\Delta G$  at 298, 308 and 318 K indicated that the adsorption process was spontaneous in nature. The positive value of  $\Delta H$  (3.48 kJ/mol) was below 20.9 kJ/mol, suggesting that the adsorption reaction was the physisorption and endothermic process<sup>[24]</sup>. The positive value of  $\Delta S$  suggested that the randomness at the solid/liquid interface increased

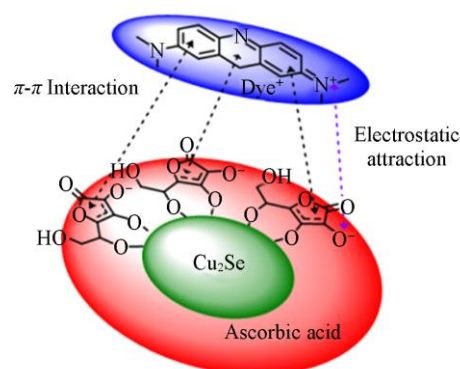


**Fig.4** Schematic illustration of the adsorption mechanism for MB on Cu<sub>2</sub>SeNPs

during the adsorption of MB on Cu<sub>2</sub>SeNPs.

**Table 3** Values of thermodynamic parameters for MB adsorption on Cu<sub>2</sub>SeNPs\*

T/K	$\Delta G/(\text{kJ}\cdot\text{mol}^{-1})$	$\Delta H/(\text{kJ}\cdot\text{mol}^{-1})$	$\Delta S/(\text{J}\cdot\text{mol}^{-1}\cdot\text{K}^{-1})$
298	-17.62	3.48	70.75
308	-18.29		
318	-19.04		

\*  $\ln K_L=8.6-0.45/T$ ,  $r^2=0.98$ .

### 3.5 Adsorption Kinetics

The kinetic analysis of adsorption process can provide essential information on the elucidation of adsorption mechanism and the dye's uptake rate. The pseudo-first-order, pseudo-second-order and intraparticle diffusion models were applied to the experimental data obtained. The linearization of three kinetic models is presented in Fig.5. The kinetic parameters and the correlation coefficients are listed in Table 4. The correlation coefficients of pseudo-second-order model are much higher than those of the other two models. Furthermore, the  $Q_{e,cal}$  values of pseudo-second-order agreed very well with the experimental ones. The results implied that the kinetics of MB adsorption on Cu<sub>2</sub>SeNPs followed the pseudo-second-order kinetic model.

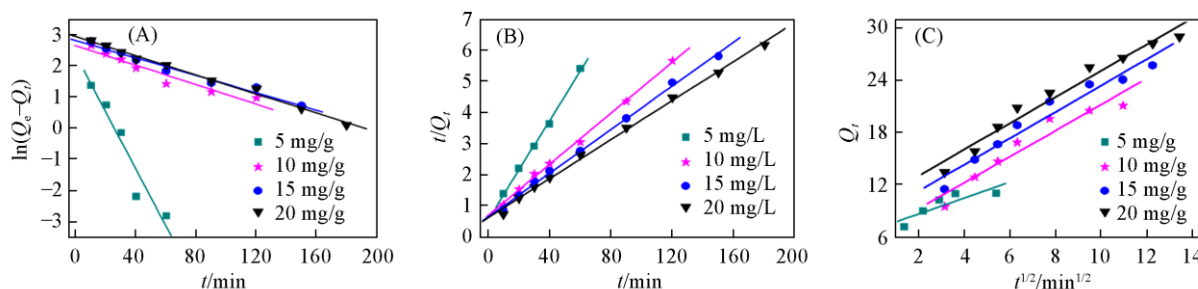


**Fig.5** Linearization of adsorption kinetics

(A) Pseudo first-order model; (B) pseudo-second-order model; (C) intraparticle diffusion model of MB adsorption on Cu<sub>2</sub>SeNPs.

**Table 4** Kinetic parameters for MB adsorption on Cu<sub>2</sub>SeNPs\*

$c_0$ /(mg·g <sup>-1</sup> )	$Q_{e,exp}$ /(mg·g <sup>-1</sup> )	Pseudo-first order			Pseudo-second-order			Intraparticle diffusion		
		$Q_{e,cal}$ /(mg·g <sup>-1</sup> )	$k_1$ /min <sup>-1</sup>	$r^2$	$Q_{e,cal}$ /(mg·g <sup>-1</sup> )	$k_2$ /min <sup>-1</sup>	$r^2$	$k_{id}$ /min <sup>-1/2</sup>	$c$ /(mg·g <sup>-1</sup> )	$r^2$
5.0	11.1	10.1	0.09144	0.924	12.6	0.1399	0.997	0.8757	5.0	0.878
10.0	23.1	14.0	0.01559	0.933	24.3	0.05889	0.998	1.503	6.3	0.919
15.0	27.9	16.6	0.01395	0.976	28.5	0.05384	0.998	1.421	11.2	0.935
20.0	30.2	18.7	0.01531	0.974	31.8	0.05040	0.997	1.516	10.0	0.967

\*  $k_1$ (min<sup>-1</sup>) and  $k_2$ (min<sup>-1</sup>): Kinetic rate constants of pseudo-first-order and pseudo-second-order, respectively;  $c$ (mg/g): intercept of linearization of adsorption kinetics;  $k_{id}$ (min<sup>-1/2</sup>): intraparticle diffusion rate constant.

### 3.6 Regeneration and Reuse of Adsorbent

The feasibility of regeneration and reuse of the adsorbent is crucial in practical applications. As shown in Fig.6, the removal rates of MB decreased from 80.4% to 70.4% for Cu<sub>2</sub>SeNPs reused in the 5th cycle, indicating that the Cu<sub>2</sub>SeNPs had good reusability. Moreover, Re-Cu<sub>2</sub>SeNPs also maintained the adsorption performance for dyes and could be reused.

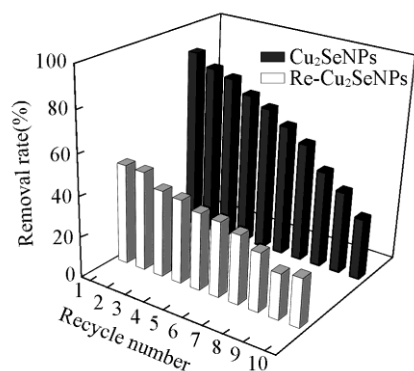


**Fig.6** Removal rates of MB in 10 cycles of adsorption-desorption

## 4 Conclusions

The surface functionalized Cu<sub>2</sub>SeNPs containing —OH and C=C group were an efficient adsorbent for both cationic (MB, RB) and anionic (MO, EY) dyes. The driving force for the adsorption of dyes was proven to be the electrostatic interactions and the  $\pi$ - $\pi$  interactions between the Cu<sub>2</sub>SeNPs and dyes. For a dose of 0.4 g/L of Cu<sub>2</sub>SeNPs, adsorption capacities of dyes were 23.1(MB), 22.9(RB) and 23.9(EY) mg/g at 298 K, an initial dye concentration of 10.0 mg/g (pH=8 for MB, pH=4 for RB and EY) and a contact time of 120 min. The adsorption of MB on Cu<sub>2</sub>SeNPs followed Langmuir isotherm and pseudo-second-order kinetic model, and was spontaneous and endothermic. Cu<sub>2</sub>SeNPs as a regenerative adsorbent had good reusability and showed great potential as a new adsorbent for organic dyes removal. More importantly, the Re-Cu<sub>2</sub>SeNPs produced from selenium nanoparticles adsorbing copper were also an efficient adsorbent for the removal of dyes. Therefore, the sequential processing of copper-containing and dyes-containing wastewaters may be feasible. The first processing would be the removal of copper by adsorption of Cu(I) on selenium nanoparticles. The second processing would be the removal of dyes by adsorption of dyes on Re-Cu<sub>2</sub>SeNPs.

## References

- [1] Dotto G. L., Santos J. M. N., Rodrigues I. L., Rosa R., Pavan F. A., Lima E. C., *J. Colloid Interface Sci.*, **2015**, 446, 133
- [2] Yagub M. T., Sen T. K., Afroze S., Ang H. M., *Adv. Colloid Interface Sci.*, **2014**, 209, 172
- [3] Chen Z., Zhang J., Fu J., Wang M., Wang X., Han R., Xu Q., *J. Hazard. Mater.*, **2014**, 273, 263
- [4] Shah V., Garg N., Madamwar D., *World J. Microbiol. Biotechnol.*, **2001**, 17(5), 499
- [5] Noubactep C., *J. Hazard. Mater.*, **2009**, 166(1), 79
- [6] Yener N., Bicer C., Onal M., Sarikaya Y., *Appl. Surf. Sci.*, **2012**, 258(7), 2534
- [7] He H., Miao Y., Du Y., Zhao J., Liu Y., Yang P., *Ceram. Int.*, **2016**, 42(1), 97
- [8] Sajab M. S., Chia C. H., Zakaria S., Khiew P. S., *Bioresour. Technol.*, **2013**, 128, 571
- [9] Widchaya R., Araya T., Ratchaneekorn W., *Chem. Res. Chinese Universities*, **2014**, 30(1), 149
- [10] Ai L., Zhang C., Liao F., Wang Y., Li M., Meng L., Jiang J., *J. Hazard. Mater.*, **2011**, 198, 282
- [11] Afkhami A., Norooz-Asl R., *Colloids and Surfaces A: Korean J. Chem. Eng.*, **2009**, 346(1), 52
- [12] Chen J., Hao Y., Liu Y., Gou J., *RSC Adv.*, **2013**, 3(20), 7254
- [13] Gui C. X., Li Q. J., Lv L. L., Qu J., Wang Q. Q., Hao S. M., Yu Z. Z., *RSC Adv.*, **2015**, 5(26), 20440
- [14] Jiang L., Zhang C., Wei J., Tjui W., Pan J., Chen Y., Liu T., *Chem. Res. Chinese Universities*, **2014**, 30(6), 971
- [15] Bai Y., Rong F., Wang H., Zhou Y., Xie X., Teng J., *J. Chem. Eng. Data*, **2011**, 56(5), 2563
- [16] Huang L., Tong X., Li Y., Teng J., Bai Y., *J. Chem. Eng. Data*, **2014**, 60(1), 151
- [17] Rong F., Bai Y., Chen T., Zheng W., *Mater. Res. Bull.*, **2012**, 47(1), 92
- [18] He G., Peng H., Liu T., Yang M., Zhang Y., Fang Y., *J. Mater. Chem.*, **2009**, 19(39), 7347
- [19] Luo J., Yu N., Xiao Z., Long C., Macharia D. K., Xu W., Zhang L., Zhu M., Chen Z., *J. Alloys Compd.*, **2015**, 648, 98
- [20] Leng L., Yuan X., Zeng G., Shao J., Chen X., Wu Z., Wang H., Peng X., *Fuel*, **2015**, 155, 77
- [21] Peng L., Qin P., Lei M., Zeng Q., Song H., Yang J., Shao J., Liao B., Gu J., *J. Hazard. Mater.*, **2012**, 209, 193
- [22] Hall K. R., Eagleton L. C., Acrivos A., Vermeulen T., *Ind. Eng. Chem. Fundam.*, **1966**, 5(2), 212
- [23] Hao Y. M., Man C., Hu Z. B., *J. Hazard. Mater.*, **2010**, 184(1), 392
- [24] Belala Z., Jeguirim M., Belhachemi M., Addoun F., Trouve G., *Desalination*, **2011**, 271(1–3), 80